Runt-Related Transcription Factor 3 Reverses Epithelial-Mesenchymal Transition in Hepatocellular Carcinoma

Shigetomi Tanaka,[1] Hidenori Shiraha,[1] Yutaka Nakanishi,[1] Shin-ichi Nishina,[1] Minoru Matsubara,[1] Shigeru Horiguchi,[1] Nobuyuki Takaoka,[1] Masaya Iwamuro,[1] Junro Kataoka,[1] Kenji Kuwaki,[1] Hiroaki Hagihara,[1] Junichi Toshimori,[1] Hideki Ohnishi,[1] Akinobu Takaki,[1] Shinichiro Nakamura,[1] Kazuhiro Nouso,[1] Takahito Yagi,[2] and Kazuhide Yamamoto[1]

From the [1]Department of Gastroenterology and Hepatology and [2]Department of Gastroenterological Surgery, Transplant, and Surgical Oncology, Okayama University Graduate School of Medicine and Dentistry, Okayama, Japan.

Short Title: RUNX3 reverses EMT in HCC

Address correspondence to: Hidenori Shiraha, MD, PhD, Department of Gastroenterology and Hepatology, Okayama University Graduate School of Medicine and Dentistry, 2-5-1 Shikata-cho, Okayama 700-8558, Japan. E-mail: hshiraha@md.okayama-u.ac.jp; Phone: +81-86-235-7219; Fax: +81-86-225-5991.

Keywords: cell migration, tumor invasion, jagged-1, E-cadherin, N-cadherin

Abbreviations: HCC, hepatocellular carcinoma; EMT, epithelial-mesenchymal transition; TWIST1, twist homolog 1; RUNX3, runt-related transcription factor 3; JAG1, jagged-1; DMEM, Dulbecco's modified Eagle's medium; FBS, fetal bovine serum; PBS, phosphate-buffered saline; SDS, sodium dodecyl sulfate; PAGE, polyacrylamide gel electrophoresis; TBS-T, tris-buffered saline with Tween 20; PCR, polymerase chain reaction; CAT, chloramphenicol acetyltransferase; MTT, 3-(4,5-dimethylthiazol-2-yl)-2,5-diphenyltetrazolium bromide; DAPI, 4′,6-diamidine-2′-phenylindole dihydrochloride; GFP, green fluorescent protein.

Appropriate article category: Cancer Cell Biology

The novelty and impact of the paper: In the present study, we demonstrate that the loss of RUNX3 expression contributes to the development of HCC. We also demonstrate a novel mechanism by which the loss of RUNX3 reduces epithelial-mesenchymal transition via decreasing jagged-1 expression.

Authorship note: Shigetomi Tanaka and Hidenori Shiraha contributed equally to this work.

Word count: 4988 words

Total number of figures and tables: 6 figures, 1 supplemental figure, and 1 supplemental table.

Total number of references: 50

Abstract

Loss or decreased expression of runt-related transcription factor 3 (RUNX3), a tumor suppressor gene involved in gastric and other cancers, has been frequently observed in hepatocellular carcinoma (HCC). The objective of this study was to identify the regulatory mechanism of the epithelial-mesenchymal transition (EMT) by RUNX3 in HCC. Human HCC cell lines, Hep3B, Huh7, HLF, and SK-Hep1, were divided into low- and high-EMT lines, based on their expression of TWIST1 and SNAI2, and were used in this *in vitro* study. Ectopic RUNX3 expression had an anti-EMT effect in low-EMT HCC cell lines characterized by increased E-cadherin expression and decreased N-cadherin and vimentin expression. RUNX3 expression has previously been reported to reduce JAG1 expression; therefore, JAG1 ligand peptide was employed to re-induce EMT in RUNX3-expressing low-EMT HCC cells. Immunohistochemical analyses were performed for RUNX3, E-cadherin, N-cadherin, and TWIST1 in 33 human HCC tissues, also divided into low- and high-EMT HCC, based on TWIST1 expression. E-cadherin expression was correlated positively and N-cadherin expression was correlated negatively with RUNX3 expression in low-EMT HCC tissues. Correlations between EMT markers and RUNX3 mRNA expression were analyzed using Oncomine datasets. Similarly, mRNA expression of E-cadherin was also significantly correlated with that of RUNX3 in low-EMT HCC, while mRNA expression of JAG1 was negatively correlated with that of RUNX3. These results suggest a novel mechanism by which loss or decreased expression of RUNX3 induces EMT via induction of JAG1 expression in low-EMT HCC.

Introduction

Hepatocellular carcinoma (HCC) is a human cancer with a high mortality rate worldwide [1-3]. Although the prognosis for HCC has improved in recent years, the prognosis for advanced disease remains poor [4-9]. Tumor progression in HCC is associated with altered expression of multiple molecules, including growth factors and their receptors, oncogenes, tumor suppressor genes, and transcription factors [1, 10]. Gaining a better understanding of the molecular mechanisms underlying tumor progression would aid in the development of new therapies for advanced HCC.

The epithelial-mesenchymal transition (EMT) is considered a critical event in the malignant transformation of cancer, especially during metastasis [11, 12]. Several models demonstrating the contribution of EMT to the progression of established tumors in transformed cells have been developed [12-14], including HCC cells [15]. Because EMT is characterized by loss of cell-cell adhesion and leads to cell individualization, EMT is known to be involved in increasing cell motility. Normally, adherent junctions connect cells via homotypic interactions mediated by E-cadherin molecules, the prototypic member of the cadherin superfamily. Not surprisingly, therefore, an inverse correlation has been found between expression of E-cadherin and the invasive capacity of a cell [16]. The downregulation of E-cadherin expression is also a major hallmark of EMT and is closely related to the malignant progression of HCC. Loss of E-cadherin expression has been strongly implicated in the progression and metastasis of human cancers [17-19]. In addition, abnormal expression of E-cadherin is a useful prognostic factor in patients with gastric carcinoma. E-cadherin

expression has also been found to be inversely correlated with the expression of certain transcription factors, including slug (SNAI2), snail (SNAI1), and twist homolog 1 (TWIST1) [20-22]. EMT is induced by several oncogenic pathways, including Src, Ras, Ets, integrin, transforming growth factor-β1, laminin 5, Wnt/β-catenin, and Notch [23-25]. The process is induced by a complex orchestration of signaling cascades comprising many signaling pathways, making the understanding of its mechanism more challenging.

The transcriptional factor TWIST1 has been shown to play a key role in EMT and metastasis in HCC [15, 20], and was originally identified as a master regulator of embryonic morphogenesis [26-28]. Recent studies have also revealed that TWIST1-induced EMT enhances tumor metastasis [29, 30], and TWIST1 expression enhanced cell migration activity in HCC cell lines [15]. Thus, here, HCC cell lines were divided into low- and high-EMT groups based on SNAI2 and TWIST1 expression.

Runt-related transcription factor 3 (RUNX3) has been reported to be a tumor suppressor gene for gastric cancer [31]. Therefore, it is not surprising that *RUNX3* gene expression decreases in HCC and other human malignancies, including those of the colon, lung, pancreas, and bile duct [32-35]. Several authors have reported that *RUNX3* gene and protein expression is decreased in HCC and that loss of RUNX3 expression prevented apoptosis in HCC cells [36-39]. We also reported that ectopic RUNX3 expression deactivated Notch signaling by decreasing jagged-1 (JAG1) expression in HCC [40]. Based on the morphological changes in an HCC cell line with ectopic RUNX3 expression, we

hypothesized that RUNX3 increases cell-cell adhesion in HCC cells. In the present study, we demonstrate that the loss of RUNX3 protein expression results in an EMT-like change via increased expression of JAG1 in HCC.

Material and Methods

Cell lines and culture. The human HCC cell lines Hep3B, Huh7, HLF, and SK-Hep1 were obtained from the American Type Culture Collection (Manassas, VA). The cells were maintained in Dulbecco's modified Eagle's medium (Invitrogen, Carlsbad, CA), supplemented with 10% heat-inactivated fetal bovine serum (FBS) (Sigma, St. Louis, MO), 1% nonessential amino acids (Sigma), 1% sodium pyruvate (Sigma), and 1% penicillin/streptomycin solution (Sigma). The cells were cultured at 37 °C in an atmosphere of 5% CO_2 and 95% air. The cells were quiesced at subconfluence under restricted serum conditions with 0.1% dialyzed FBS for 36 h before the experiment, if needed.

Immunoblot analysis. Cells were plated in 6-well, plastic tissue culture dishes and grown to confluence. The cells were washed twice with cold phosphate-buffered saline (PBS) and lysed in 150 μL of sample buffer (100 mM Tris-HCl [pH 6.8], 10% glycerol, 4% sodium dodecyl sulfate [SDS], 1% bromophenol blue, and 10% β-mercaptoethanol). The samples were resolved by SDS-polyacrylamide gel electrophoresis (PAGE), and transferred to an Immobilon-P^{TM} polyvinylidene difluoride membrane (Millipore Corporation, Bedford, MA). The membranes were blocked using Tris-buffered saline with Tween 20 (TBS-T) (Sigma) buffer containing 5% bovine serum albumin for 1 h. The membranes were then

incubated with antibodies against SNAI2 (#9589; Cell Signaling Technology, Danvers, MA), TWIST1 (sc-6269; Santa Cruz Biotechnology Inc., Santa Cruz, CA), RUNX3 (R3-G54; Abcam, Cambridge, MA), E-cadherin (#610181; BD Biosciences, San Diego, CA), N-cadherin (#05-915; Millipore), vimentin (ab8069; Abcam), and α-actin (Sigma) overnight at 4 °C. The membranes were washed 3 times with TBS-T and probed with horseradish peroxidase-conjugated secondary antibody before being developed with an ECL western blotting detection system (Amersham Biosciences, Piscataway, NJ) using enhanced chemiluminescence.

RUNX3-expressing cell lines. The human *RUNX3* construct was obtained by reverse transcriptase polymerase chain reaction (PCR)-based cloning from normal human hepatocytes [38]. The human *RUNX3* and/or chloramphenicol acetyltransferase (*CAT*) (mock) constructs were transfected into Hep3B, Huh7, HLF, or SK-Hep1 cells using the FuGene^{TM}6 transfection reagent (Roche Diagnostics, Basel, Switzerland), per the manufacturer's instructions. Forty-eight hours after transfection, cells were grown in complete medium, containing 250 μg/mL hygromycin (Roche Diagnostics). Polyclonal lines consisting of >20 colonies were established. At least 2 independent transfections were performed for each cell line, with a transfection efficiency of more than 80%, as determined by immunocytochemistry using anti-CAT antibody and/or anti-RUNX3 antibody. After selection, all experiments were performed within 5 passages to avoid natural transformation and natural selection. The cells were cultured under serum-starved conditions for 24–36 h, if needed, and utilized in the following experiments.

Morphological analysis. Cells were plated onto 6-well, plastic tissue culture dishes with quiescent medium at a density of 10^5 cells/mL. After 24 h, morphological observations were made using phase-contrast microscopy (IMT-2; Olympus, Tokyo, Japan).

Immunocytochemistry analysis. Cells were cultured in a glass chamber (Lab-Tek II; Nalgene Nunc, Roskilde, Denmark) to a density of approximately 2×10^5 cells/mL for 24 h, prior to being fixed for 20 min in 3% freshly hydrolyzed paraformaldehyde in PBS, at room temperature. After washing with PBS, the cells were incubated with anti-E-cadherin antibody (M3613, Dako Japan, Tokyo, Japan) for 30 min at room temperature, and visualized using Oregon Green-conjugated secondary antibody (Invitrogen). Photographs were taken using a fluorescence microscope (BX51, Olympus) equipped with a digital image capturing system (DP50, Olympus).

MTT assay. Cell proliferation activity was assessed using a 3-(4,5-dimethylthiazol-2-yl)-2,5-diphenyltetrazolium bromide (MTT) (Sigma) assay. In brief, cells were grown in 96-well tissue culture dishes. After 24 h of quiescence, the cells were cultured for the indicated period with or without 10% FBS. At the end of the treatment, 10 µL of MTT (5 mg/mL in PBS) was added to each well and incubated for an additional 4 h at 37 °C. The purple-blue MTT formazan precipitate was dissolved in 100 µL of isopropanol/HCl (0.04 N). The activity of the mitochondria, reflecting cellular growth and viability, was evaluated by measuring the optical density at 570 nm with a microplate

reader (Bio-Rad, Hercules, CA).

Cell migration assay. Cell migration was assessed using an *in vitro* wound healing assay. The cells were cultured in 6-well tissue culture dishes. After 24 h of quiescence, experimental wounds were made by dragging a rubber Policeman™ (Fisher Scientific, Hampton, NH) across the cell culture. The cultures were rinsed with PBS and placed in fresh quiescence medium. The cells were treated with 10% FBS and/or caspase inhibitor (Caspase Inhibitor IV, 100 μM; Calbiochem, Gibbstown, NJ) for 24 h at 37 °C. Three wounds were created for each specimen. Photographs were taken at 0 and 24 h, and the relative distance traveled by the cells at the acellular front was determined.

DAPI staining. Cells were grown to 50% confluence in a glass chamber (Lab-Tek II; Nalgene Nunc) and quiesced for 24 h. The cells were then treated with 10% FBS and/or caspase inhibitor IV (100 μM) for 24 h. Following exposure, chromosomal DNA was stained with 4′,6-diamidino-2-phenylindole dihydrochloride (DAPI; Dojindo, Kumamoto, Japan), at a concentration of 1 μg/mL in PBS for 2 min, according to the manufacturer's protocol. The stained cells were then observed by fluorescence microscopy (IX-70; Olympus).

Ectopic* TWIST1 *protein expression. Human *TWIST1* cDNA was obtained by PCR-based cloning from a normal human placenta cDNA library (Takara Bio Inc., Otsu, Japan) and subcloned into the pcDNA 3.1 expression vector (Invitrogen) [15]. *TWIST1* and green

fluorescent protein (GFP; control) constructs were transfected into RUNX3-expressing Hep3B cells using Fugene^{TM}6 (Roche Diagnostics). Cells were incubated for 48 h after transfection, after which immunoblot analyses and the cell migration assays were performed.

JAG1 ligand treatment. Because RUNX3 expression deactivates Notch signaling by downregulating JAG1 expression [40], the JAG1 ligand peptide was employed to activate Notch signaling [41]. RUNX3- or control CAT-expressing Hep3B cells were treated with or without 50 μM JAG1 ligand peptide (AnaSpec, Fremont, CA) and/or control-scrambled peptide for 48 h. Cells were then lysed and an immunoblot analysis was performed.

HCC tissues and immunohistochemistry. A group of 33 patients, 24 men (age range, 39–77 years; average age, 62.2 years), and 9 women, (age range, 54–82 years; average age, 64.9 years), were included in this study. Resected HCC tissues were obtained after receiving written informed consent that adhered to the stringent ethical criteria of the Okayama University Graduate School of Medicine, Dentistry and Pharmaceutical Sciences. Immunohistochemistry was performed on formalin-fixed paraffin sections prepared from the resected tissue. Sections were dewaxed and dehydrated; after rehydration, endogenous peroxidase activity was blocked for 30 min in a methanol solution containing 0.3% hydrogen peroxide. Following antigen retrieval in citrate buffer, the sections were blocked, again, overnight at 4 °C. The sections were probed with anti-RUNX3 rabbit polyclonal antibody (ab49117; Abcam), anti-E-cadherin monoclonal antibody (Dako Japan),

anti-N-cadherin monoclonal antibody (M3613; Dako Japan), anti-SNAI2 rabbit polyclonal antibody (#9585; Cell Signaling Technology), and anti-TWIST1 goat polyclonal antibody (Santa Cruz Biotechnology, Inc.). The primary antibody was detected using a biotinylated anti-rabbit antibody (Dako Japan) or a biotinylated anti-goat antibody (Dako Japan). The signal was amplified by avidin-biotin complex formation and was developed with diaminobenzidine, followed by dehydration in alcohol and xylene, and the sections were mounted. The sections were scored for RUNX3, E-cadherin, N-cadherin, and TWIST1 expression using a 4-point scale: 0, negative; 1, weak signal; 2, intermediate signal; and 3, strong signal [42]. All sections were scored independently by 2 observers, without prior knowledge of the clinical background. All discrepancies in scoring were reviewed and a consensus was reached. Because TWIST1 is a major EMT inducer and an indicator [43], TWIST1-positive (score 2 or 3) HCCs were designated as high-EMT HCCs, while TWIST1-negative (score 0 or 1) HCCs were designated as low-EMT HCCs. The clinicopathological features, TWIST1, and RUNX3 expression levels are shown in the Supplemental Table 1. Statistical analyses were performed using JMP software (SAS Institute Inc., Cary, NC).

Gene expression profiling analysis in human HCC. To further investigate correlations between RUNX3 expression and transcriptional regulation of E-cadherin, N-cadherin, and vimentin, *JAG1* expression profiles in low-EMT HCCs from publicly available HCC data sets were evaluated using Oncomine (hppt://www.oncomine.org). In brief, after excluding *TWIST1*-positive (high-EMT) (*TWIST1*/213943_at > -0.20) HCCs from the Chiang Liver

data sets, mRNA expression profiles for *RUNX3*, E-cadherin, N-cadherin, vimentin, and *JAG1* were evaluated using *RUNX3*/234928_x_at, *CDH1*/201130_s_at, *CDH2*/203440_at, *VIM*/155938_x_at, and *JAG1*/231183_s, respectively. Statistical analyses were performed using JMP software (SAS Institute Inc.).

Results

EMT-inducer expression in HCC cell lines. HCC cell lines were divided into 2 groups according to SNAI2 and TWIST1 expression: Hep3B and Huh7 cells were designated as low-EMT cells, and HLF and SK-Hep1 cells as high-EMT cells (Fig. 1). Low-EMT cells expressed E-cadherin, while no detectable level of E-cadherin was found in high-EMT cells.

Ectopic RUNX3 expression in HCC cell lines. Ectopic RUNX3 expression was evaluated in endogenous RUNX3-negative HCC cell lines [38], and the morphological changes were analyzed under phase-contrast microscopy. Ectopic RUNX3 expression changed the morphology of the cells from a fibroblast-like spindle shape to a paving stone, sheet-like structure in Hep3B (Fig. 2A) and Huh7 cells (Supplemental Fig. 1). These cells showed well-organized cell-cell adhesion, characteristic of epithelial cells. E-cadherin expression was enhanced in the RUNX3-expressing Hep3B cells (Fig. 2B) or Huh7 cells (data not shown), especially at the cell-cell junction. In contrast, RUNX3 expression did not induce significant morphological changes in HLF (Fig. 2A) or SK-Hep1 cells (Supplemental Fig. 1), neither was E-cadherin expression significantly different in these cells (Fig. 2B).

RUNX3 protein expression was also confirmed in *RUNX3* cDNA-transfected cells (Fig. 2C).

Ectopic RUNX3 protein expression inverted EMT in HCC cell lines. E-cadherin, N-cadherin, and vimentin expression were assessed by immunoblot analysis in HCC cell lines (Fig. 2C). E-cadherin expression was induced by ectopic RUNX3 protein expression in low-EMT cells. High-EMT HCC cells did not express E-cadherin, and ectopic RUNX3 protein expression did not induce E-cadherin expression and it had little effect on N-cadherin and vimentin expression in high-EMT HCC cells. However, ectopic RUNX3 protein expression suppressed N-cadherin and vimentin expression in low-EMT HCC cells.

Ectopic RUNX3 protein expression suppressed cell growth under serum starvation. To confirm the biological effects of ectopic RUNX3 protein expression, MTT assays were performed to determine the effect on cell proliferation. In all 4 HCC cell lines, RUNX3 expression suppressed cell growth by 31–38% (Fig. 2D).

Ectopic RUNX3 protein expression suppressed cell migration in HCC cell lines. The effect of ectopic RUNX3 expression on HCC cell lines was examined in the *in vitro* wound healing assay, which is commonly used to assess the effects of pro- and anti-migratory agents on cultured cells. RUNX3 expression significantly suppressed cell migration by 70% ± 20% and 63% ± 5% in Hep3B and Huh7 cells, respectively, but not in HLF and SK-Hep1 cells (Fig. 2E).

Effect of RUNX3 expression on cell migration in the presence of an apoptosis inhibitor. An apoptosis inhibitor was used to determine if apoptosis-inducing factors affected cell migration activity in ectopic RUNX3 protein-expressing HCC cell lines. Caspase inhibitor IV was observed to inhibit serum starvation-induced apoptosis by 74% in RUNX3-expressing Hep3B cells (Fig. 3A). However, caspase inhibitor IV did not abrogate the RUNX3-induced reduction in cell migration activity in these cells (Fig. 3B).

TWIST1 expression abrogated the anti-EMT effect of ectopic RUNX3. RUNX3 appeared to have a weak effect on EMT in TWIST1-positive HCC cell lines. To determine if ectopic TWIST1 expression affects the anti-EMT effect of RUNX3 expression, TWIST1 cDNA was introduced into the TWIST1-negative HCC cell line Hep3B, causing the cells to transiently express TWIST1 (Fig. 4A). RUNX3 expression did not have a significant effect on the EMT markers, E-cadherin, N-cadherin, or vimentin in TWIST1-expressing Hep3B cells (Fig. 4A). Likewise, RUNX3 expression did not have the anti-migratory effect on TWIST1-expressing Hep3B cells (Fig. 4B).

JAG1 expression. The JAG1 ligand peptide was used to determine if RUNX3 expression is regulated via JAG1. The JAG1 ligand peptide decreased E-cadherin expression in RUNX3-expressing Hep3B cells (Fig. 5) and induced re-expression of N-cadherin and vimentin in RUNX3-expressing Hep3B cells (Fig. 5).

E-cadherin expression correlation with RUNX3 expression in HCC tissues. Thirty-three HCC tissue samples were available for comparing E-cadherin and RUNX3 protein expression by immunohistochemistry. Representative images of E-cadherin-negative (Score 0), E-cadherin-positive (Score 3), N-cadherin-negative (Score 0), and N-cadherin-positive (Score 3) tissues are shown in Figs. 6A-a, b, c, and d, respectively. To determine if there was a relationship between E-cadherin and RUNX3 expression in HCC tissues, the scores for E-cadherin immunoreactivity were plotted against those for RUNX3 (Fig. 6B). In general, low E-cadherin expression scores were observed in tissues with low RUNX3 expression. Statistical analysis revealed that RUNX3 expression and E-cadherin expression were significantly correlated ($r = 0.58$, $P = 0.0025$) in low-EMT HCC tissues. Scores for N-cadherin immunoreactivity were also plotted against those for RUNX3 (Fig. 6C), where high N-cadherin expression scores were observed in tissues with low RUNX3 expression. A significant inverse correlation was found between RUNX3 and N-cadherin expression ($r = -0.74$, $P < 0.0001$). Thus, high-EMT HCC tissues showed low expression of E-cadherin and high expression of N-cadherin.

Gene expression profiling analysis in human HCC. A further examination of the correlation between expression of RUNX3 and of EMT markers was conducted by analyzing the Oncomine datasets. These analyses revealed that *JAG1* mRNA expression was negatively correlated with *RUNX3* mRNA expression in low-EMT HCC tissues ($r = 0.28$, $P < 0.05$) (Fig. 6D). E-cadherin mRNA expression was also found to be significantly correlated with *RUNX3* mRNA expression in low-EMT HCC tissues ($r = 0.33$, $P < 0.05$)

(Fig. 6D). mRNA expressions of N-cadherin and vimentin tended to be negatively correlated with *RUNX3* mRNA expression, but the correlations were not significant (r = -0.24 and -0.07, respectively) (Fig. 6D).

Discussion

RUNX3 expression is generally reduced in human HCC tissues [36, 38]. However, the role of decreased RUNX3 expression in the development and progression of HCC has not yet been fully elucidated. The results obtained here suggest that decreased expression of the RUNX3 protein contributes to induction of EMT in HCC cell lines.

Ectopic RUNX3 expression was evaluated in the endogenous RUNX3-negative HCC cell lines Hep3B, Huh7, HLF, and SK-Hep1 (Fig. 2C). The establishment of RUNX3-expressing cell lines was advantageous in order to elucidate the RUNX3-related molecular mechanism, as they helped to provide additional clarity to the results obtained. RUNX3 expression is known to cause apoptosis, especially in the absence of FBS [38], whereas RUNX3-expressing cells can grow in the presence of FBS. Because RUNX3 is a strong apoptosis inducer [38, 44], the anti-cell migratory effect of RUNX3 could be due to the apoptosis enhanced by serum starvation. Therefore, a caspase inhibitor was employed to eliminate the potential effects of apoptosis on cell migration. The caspase inhibitor successfully abrogated RUNX3-induced apoptosis (Fig. 3A), but RUNX3-expressing cells did not recover their cell migration activity (Fig. 3B). Morphological studies also showed that ectopic RUNX3 expression induced phenotypic changes, resulting in the cells adopting

a more plate-like shape instead of their normal, spindle-like shape, in the low-EMT HCC cell lines, but not in the high-EMT HCC cell lines. These results are consistent with the cell shapes generally associated with migratory and non-migratory cells. Collectively, these results suggest that RUNX3 is directly connected to the inhibition of cellular migration associated with metastatic cells.

Several studies examined the downregulation of E-cadherin in HCCs by immunohistochemical analyses [44-46]. In accordance with these reports, E-cadherin expression was generally reduced in human HCC tissues and was correlated with RUNX3 expression (Fig. 6B). The strong correlation between RUNX3 and E-cadherin expression suggests that loss of RUNX3 expression may cause reduced E-cadherin expression. Similarly, RUNX3 was only able to induce E-cadherin expression in low-EMT HCC cell lines (Fig. 2B, 2C). As TWIST1 is a strong inducer of EMT and reduces E-cadherin expression, RUNX3 had no effect on E-cadherin expression and very little effect on N-cadherin and vimentin expression in high-EMT cells (Fig. 2C). But, N-cadherin and vimentin expression were reduced by ectopic RUNX3 expression in low-EMT HCC cells. Expression of N-cadherin was also analyzed in human HCC tissues. N-cadherin expression was inversely related to RUNX3 expression in low-EMT HCC tissues (Fig. 6C).

The effects of TWIST1 expression on RUNX3-expressing HCC cell lines were examined by transiently expressing the TWIST1 protein in TWIST1-negative Hep3B cells by transfecting *TWIST1* cDNA into CAT- and RUNX3-expressing Hep3B cells (Fig. 4A).

Ectopic RUNX3 protein expression did not have a significant effect on the EMT markers and cell migration activity in TWIST1-expressing cells (Fig. 4B). Although there is a possibility that TWIST1 and RUNX3 independently act on E-cadherin, N-cadherin, and vimentin expression, the present results suggest that TWIST1 is the more important regulator of these EMT markers. Therefore, a sequence of genetic alterations in the progression of EMT in HCC may be hypothesized based on the frequency of gene alteration in HCC. The loss of RUNX3 protein expression was found in ~90% of HCC tissue samples, while TWIST1 expression was found in ~30% of HCC tissue samples [15, 38]. Recently, Aleksic et al. also reported that loss of RUNX3 was a frequent, early event in chemical liver carcinogenesis [47]. Various authors have reported that a loss of or decreased expression of RUNX3 is generally found in HCC [37-39], suggesting that decreased expression of RUNX3 could be an early event in human HCC. Since TWIST1 expression reduced RUNX3 expression (Fig. 4A), TWIST1 may interact with RUNX3 to progress EMT in HCC. Further studies are needed to elucidate the detailed mechanism of interaction between RUNX3 and TWIST1 expression.

RUNX3 has also been previously reported to regulate JAG1 expression in HCC cells by suppressing transcription through direct binding to the transcriptional regulatory region of JAG1 [40]. To clarify whether RUNX3 regulates EMT in HCC cells through JAG1 expression, the JAG1 ligand peptide was employed. The JAG1 ligand peptide successfully re-induced EMT in RUNX3-expressing Hep3B cells (Fig. 5).

Because a relatively small number of HCC tissues were analyzed for RUNX3 and EMT marker expression using immunohistochemistry, Oncomine datasets were also analyzed for *RUNX3* mRNA expression and the mRNA of EMT markers in low-EMT HCCs (Fig. 6D). In accordance with both a previous report [40] and the present results, *JAG1* mRNA expression was significantly, negatively correlated with *RUNX3* mRNA expression (Fig. 6D) and E-cadherin mRNA expression was significantly correlated with *RUNX3* mRNA expression (Fig. 6D). Although significant correlations were not found between *RUNX3* mRNA expression and the other EMT markers, N-cadherin mRNA expression and vimentin mRNA expression tended to be inversely related to *RUNX3* mRNA expression.

A repressive function of EMT has been found in a study of tumor suppressor genes in which depletion of a retinoblastoma protein induced EMT in a breast cancer cell line [48]. The present study suggests that other tumor suppressor genes may be similarly involved in EMT. A relationship between RUNX3 expression and EMT was reported by Chang et al., who demonstrated that RUNX3 expression induced claudin expression [49]. The regulatory function of EMT by RUNX3 was also predicted in a prospective review [50]. Herein, we demonstrated that RUNX3 expression regulates EMT through JAG1 expression.

Conclusions

We uncovered a novel function of RUNX3 in regulating EMT in HCC. Our results suggest that loss or decreased expression of RUNX3 induced EMT via inducing JAG1 expression.

Acknowledgments

The authors wish to thank Tatsuya Fujikawa for valuable suggestions.

Financial support: This work is supported by a grant-in-aid from the Japan Society for the Promotion of Science (Grant #23590975).

Potential conflict of interest: Nothing to report.

References

1. El-Serag HB, Rudolph KL. Hepatocellular carcinoma: epidemiology and molecular carcinogenesis. *Gastroenterol* 2007;**132**:2557-76.
2. Garcia M, Jernal A, Ward EM, Center MM, Hao Y, Siegel RI, Thun MJ, Global Cancer Facts & Figures 2007,.2007; Society AC. Atlanta, GA
3. Parkin DM, Bray F, Ferlay J, Pisani P. Estimating the world cancer burden: Globocan 2000. *Int J Cancer* 2001;**94**:153-6.
4. Kaizu T, Karasawa K, Tanaka Y, Matuda T, Kurosaki H, Tanaka S, Kumazaki T. Radiotherapy for osseous metastases from hepatocellular carcinoma: a retrospective study of 57 patients. *Am J Gastroenterol* 1998;**93**:2167-71.
5. Patt YZ, Claghorn L, Charnsangavej C, Soski M, Cleary K, Mavligit GM. Hepatocellular carcinoma. A retrospective analysis of treatments to manage disease confined to the liver. *Cancer* 1988;**61**:1884-8.
6. Stuart KE, Anand AJ, Jenkins RL. Hepatocellular carcinoma in the United States. Prognostic features, treatment outcome, and survival. *Cancer* 1996;**77**:2217-22.
7. Falkson G, MacIntyre JM, Moertel CG, Johnson LA, Scherman RC. Primary liver cancer. An Eastern Cooperative Oncology Group Trial. *Cancer* 1984;**54**:970-7.
8. Doci R, Bignami P, Bozzetti F, Bonfanti G, Audisio R, Colombo M, Gennari L. Intrahepatic chemotherapy for unresectable hepatocellular carcinoma. *Cancer* 1988;**61**:1983-7.
9. Okuda K, Ohtsuki T, Obata H, Tomimatsu M, Okazaki N, Hasegawa H, Nakajima Y, Ohnishi K. Natural history of hepatocellular carcinoma and prognosis in relation to treatment. Study of 850 patients. *Cancer* 1985;**56**:918-28.
10. Coleman WB. Mechanisms of human hepatocarcinogenesis. *Curr Molec Med* 2003;**3**:573-88.
11. Arias AM. Epithelial mesenchymal interactions in cancer and development. *Cell* 2001;**105**:425-31.
12. Thiery JP. Epithelial-mesenchymal transitions in tumour progression. *Nature* reviews 2002;**2**:442-54.
13. Laffin B, Wellberg E, Kwak HI, Burghardt RC, Metz RP, Gustafson T, Schedin P, Porter WW. Loss of singleminded-2s in the mouse mammary gland induces an epithelial-mesenchymal transition associated with up-regulation of slug and matrix metalloprotease 2. *Molec Cell Biol* 2008;**28**:1936-46.

14. Huber MA, Kraut N, Beug H. Molecular requirements for epithelial-mesenchymal transition during tumor progression. C*urr Opinion Cell Biol* 2005;**17**:548-58.
15. Matsuo N, Shiraha H, Fujikawa T, Takaoka N, Ueda N, Tanaka S, Nishina S, Nakanishi Y, Uemura M, Takaki A, Nakamura S, Kobayashi Y, et al. Twist expression promotes migration and invasion in hepatocellular carcinoma. *Cancer* 2009;**9**:240.
16. Frixen UH, Behrens J, Sachs M, Eberle G, Voss B, Warda A, Lochner D, Birchmeier W. E-cadherin-mediated cell-cell adhesion prevents invasiveness of human carcinoma cells. *J Cell Biol* 1991;**113**:173-85.
17. Umbas R, Schalken JA, Aalders TW, Carter BS, Karthaus HF, Schaafsma HE, Debruyne FM, Isaacs WB. Expression of the cellular adhesion molecule E-cadherin is reduced or absent in high-grade prostate cancer. *Cancer Res* 1992;**52**:5104-9.
18. Cleton-Jansen AM, Moerland EW, Kuipers-Dijkshoorn NJ, Callen DF, Sutherland GR, Hansen B, Devilee P, Cornelisse CJ. At least two different regions are involved in allelic imbalance on chromosome arm 16q in breast cancer. *Genes Chromosomes Cancer* 1994;**9**:101-7.
19. Carter BS, Ewing CM, Ward WS, Treiger BF, Aalders TW, Schalken JA, Epstein JI, Isaacs WB. Allelic loss of chromosomes 16q and 10q in human prostate cancer. *Proc Nat Acad Sci USA* 1990;**87**:8751-5.
20. Lee TK, Poon RT, Yuen AP, Ling MT, Kwok WK, Wang XH, Wong YC, Guan XY, Man K, Chau KL, Fan ST. Twist overexpression correlates with hepatocellular carcinoma metastasis through induction of epithelial-mesenchymal transition. *Clin Cancer Res* 2006;**12**:5369-76.
21. Jiao W, Miyazaki K, Kitajima Y. Inverse correlation between E-cadherin and Snail expression in hepatocellular carcinoma cell lines in vitro and in vivo. *Br J Cancer* 2002;**86**:98-101.
22. Thiery JP. Epithelial-mesenchymal transitions in development and pathologies. *Curr Opinion Cell Biol* 2003;**15**:740-6.
23. Boyer B, Valles AM, Edme N. Induction and regulation of epithelial-mesenchymal transitions. *Biochem Pharmacol* 2000;**60**:1091-9.
24. Giannelli G, Bergamini C, Fransvea E, Sgarra C, Antonaci S. Laminin-5 with transforming growth factor-beta1 induces epithelial to mesenchymal transition in hepatocellular carcinoma. *Gastroenterol* 2005;**129**:1375-83.
25. van Zijl F, Zulehner G, Petz M, Schneller D, Kornauth C, Hau M, Machat G,

Grubinger M, Huber H, Mikulits W. Epithelial-mesenchymal transition in hepatocellular carcinoma. *Future Oncol* 2009;**5**:1169-79.

26. Chen ZF, Behringer RR. twist is required in head mesenchyme for cranial neural tube morphogenesis. *Genes Devel* 1995;**9**:686-99.
27. Lee MS, Lowe GN, Strong DD, Wergedal JE, Glackin CA. TWIST, a basic helix-loop-helix transcription factor, can regulate the human osteogenic lineage. *J Cell Biochem* 1999;**75**:566-77.
28. Thisse B, el Messal M, Perrin-Schmitt F. The twist gene: isolation of a *Drosophila* zygotic gene necessary for the establishment of dorsoventral pattern. *Nucleic Acids Res* 1987;**15**:3439-53.
29. Vernon AE, LaBonne C. Tumor metastasis: a new twist on epithelial-mesenchymal transitions. *Curr Biol* 2004;**14**:R719-21.
30. Yang J, Mani SA, Donaher JL, Ramaswamy S, Itzykson RA, Come C, Savagner P, Gitelman I, Richardson A, Weinberg RA. Twist, a master regulator of morphogenesis, plays an essential role in tumor metastasis. *Cell* 2004;**117**:927-39.
31. Li QL, Ito K, Sakakura C, Fukamachi H, Inoue K, Chi XZ, Lee KY, Nomura S, Lee CW, Han SB, Kim HM, Kim WJ, et al. Causal relationship between the loss of RUNX3 expression and gastric cancer. *Cell* 2002;**109**:113-24.
32. Araki K, Osaki M, Nagahama Y, Hiramatsu T, Nakamura H, Ohgi S, Ito H. Expression of RUNX3 protein in human lung adenocarcinoma: Implications for tumor progression and prognosis. *Cancer Sci* 2005;**96**:227-31.
33. Ku JL, Kang SB, Shin YK, Kang HC, Hong SH, Kim IJ, Shin JH, Han IO, Park JG. Promoter hypermethylation downregulates RUNX3 gene expression in colorectal cancer cell lines. *Oncogene* 2004;**23**:6736-42.
34. Li J, Kleeff J, Guweidhi A, Esposito I, Berberat PO, Giese T, Buchler MW, Friess H. RUNX3 expression in primary and metastatic pancreatic cancer. *J Clin Pathol* 2004;**57**:294-9.
35. Wada M, Yazumi S, Takaishi S, Hasegawa K, Sawada M, Tanaka H, Ida H, Sakakura C, Ito K, Ito Y, Chiba T. Frequent loss of RUNX3 gene expression in human bile duct and pancreatic cancer cell lines. *Oncogene* 2004;**23**:2401-07.
36. Li X, Zhang Y, Qiao T, Wu K, Ding J, Liu J, Fan D. RUNX3 Inhibits growth of HCC cells and HCC xenografts in mice in combination with adriamycin. *Cancer Biol Ther* 2008;**7**:669-76.

37. Mori T, Nomoto S, Koshikawa K, Fujii T, Sakai M, Nishikawa Y, Inoue S, Takeda S, Kaneko T, Nakao A. Decreased expression and frequent allelic inactivation of the RUNX3 gene at 1p36 in human hepatocellular carcinoma. *Liver Int* 2005;**25**:380-8.
38. Nakanishi Y, Shiraha H, Nishina SI, Tanaka S, Matsubara M, Horiguchi S, Iwamuro M, Takaoka N, Uemura M, Kuwaki K, Hagihara H, Toshimori J, et al. Loss of runt-related transcription factor 3 expression leads hepatocellular carcinoma cells to escape apoptosis. *BMC Cancer* 2011;**11**:3.
39. Xiao WH, Liu WW. Hemizygous deletion and hypermethylation of RUNX3 gene in hepatocellular carcinoma. *World J Gastroenterol* 2004;**10**:376-80.
40. Nishina S, Shiraha H, Nakanishi Y, Tanaka S, Matsubara M, Takaoka N, Uemura M, Horiguchi S, Kataoka J, Iwamuro M, Yagi T, Yamamoto K. Restored expression of the tumor suppressor gene RUNX3 reduces cancer stem cells in hepatocellular carcinoma by suppressing Jagged1-Notch signaling. *Oncol Rep* 2011;**26**:523-31.
41. Weijzen S, Velders MP, Elmishad AG, Bacon PE, Panella JR, Nickoloff BJ, Miele L, Kast WM. The Notch ligand Jagged-1 is able to induce maturation of monocyte-derived human dendritic cells. *J Immunol* 2002;**169**:4273-8.
42. Ng IO, Chung LP, Tsang SW, Lam CL, Lai EC, Fan ST, Ng M. p53 gene mutation spectrum in hepatocellular carcinomas in Hong Kong Chinese. *Oncogene* 1994;**9**:985-90.
43. Savagner P, Yamada KM, Thiery JP. The zinc-finger protein slug causes desmosome dissociation, an initial and necessary step for growth factor-induced epithelial-mesenchymal transition. *J Cell Biol* 1997;**137**:1403-19.
44. Yoshiura K, Kanai Y, Ochiai A, Shimoyama Y, Sugimura T, Hirohashi S. Silencing of the E-cadherin invasion-suppressor gene by CpG methylation in human carcinomas. *Proc Nat Acad Sci USA* 1995;**92**:7416-9.
45. Kanai Y, Ushijima S, Hui AM, Ochiai A, Tsuda H, Sakamoto M, Hirohashi S. The E-cadherin gene is silenced by CpG methylation in human hepatocellular carcinomas. *Int J Cancer* 1997;**71**:355-9.
46. Matsumura T, Makino R, Mitamura K. Frequent down-regulation of E-cadherin by genetic and epigenetic changes in the malignant progression of hepatocellular carcinomas. *Clin Cancer Res* 2001;**7**:594-9.
47. Aleksic K, Lackner C, Geigl JB, Schwarz M, Auer M, Ulz P, Fischer M, Trajanoski Z, Otte M, Speicher MR. Evolution of genomic instability in diethylnitrosamine-induced

hepatocarcinogenesis in mice. *Hepatol* 2011;**53**:895-904.

48. Arima Y, Inoue Y, Shibata T, Hayashi H, Nagano O, Saya H, Taya Y. Rb depletion results in deregulation of E-cadherin and induction of cellular phenotypic changes that are characteristic of the epithelial-to-mesenchymal transition. *Cancer Res* 2008;**68**:5104-12.
49. Chang TL, Ito K, Ko TK, Liu Q, Salto-Tellez M, Yeoh KG, Fukamachi H, Ito Y. Claudin-1 has tumor suppressive activity and is a direct target of RUNX3 in gastric epithelial cells. *Gastroenterol* 2010;**138**:255-65 e1-3.
50. Shiraha H, Nishina SI, Yamamoto K. Loss of runt-related transcription factor 3 causes development and progression of hepatocellular carcinoma. *J Cell Biochem* 2011;**112**:745-49.

Figure Legends

Fig. 1. Expression of epithelial-mesenchymal transition (EMT) inducers in hepatocellular carcinoma (HCC) cell lines. Immunoblot analyses were performed using antibodies against SNAI2, TWIST1, and E-cadherin. Immunoblotting for α-actin levels was used to verify equal loading of cellular proteins. HCC cell lines were divided into 2 groups according to EMT-inducer SNAI2 and TWIST1expression. Representative blots of more than 3 independent experiments are shown.

Fig. 2. Ectopic RUNX3 protein expression in hepatocellular carcinoma (HCC) cell lines. Eukaryotic expression constructs for CAT (mock) and RUNX3 were introduced into Hep3B, Huh7, HLF, and SK-Hep1 cell lines. After a 24-h quiescence, cells were used for the experiments in the presence of 10% FBS. (A) Micrographs were taken by phase-contrast microscopy. The micrographs are representative of 3 independent experiments. Bar = 100 μm. (B) Immunocytochemical analysis was performed using antibody against E-cadherin. The micrographs are representative of 3 independent experiments. Bar = 40 μm. (C) Immunoblot analyses were performed using antibodies against RUNX3, E-cadherin, N-cadherin, and vimentin. Immunoblotting for α-actin levels was used to verify equal loading of cellular proteins. Representative blots of more than 3 independent studies are shown. (D) Cell proliferation activity was measured by MTT assay (mock, white bars; RUNX3, black bars). (E) Cell migration activity was measured as described in the Material and Methods (mock, white bars; RUNX3, black bars). (D, E) All results were normalized to

cell proliferation and migration activity for CAT-expressing Hep3B cells. Data represent the mean ± SE of more than 3 independent experiments, each performed in triplicate. n.s., $P > 0.05$; *, $P < 0.05$; **, $P < 0.01$ (versus data for mock-transfected Hep3B); Student's *t* test.

Fig. 3. Effect of an apoptosis inhibitor. Hep3B cells were cultured on glass chamber slides and quiesced, then treated with or without caspase inhibitor IV (100 μM) and 10% fetal bovine serum. (A) Apoptosis was quantified using the DAPI apoptosis detection assay (mock, white bars; RUNX3, black bars). Results are expressed as percent apoptotic cells. Data represent the mean ± SE of more than 3 independent experiments, each performed in triplicate. n.s., $P > 0.05$; **, $P < 0.01$ (versus data for mock-transfected cells); Student's *t* test. (B) Cell migration activities were measured as described in the Material and Methods (mock, white bars; RUNX3, black bars). All results are normalized to data for untreated control cells. Data represent the mean ± SE of more than 3 independent experiments, each performed in triplicate. n.s., $P > 0.05$; *, $P < 0.05$; **, $P < 0.01$ (versus data for mock-transfected cells); Student's *t* test.

Fig. 4. Effect of TWIST1 expression on epithelial-mesenchymal transition (EMT) markers. CMV-driven eukaryotic expression constructs for green fluorescent protein (GFP; control) and TWIST1 were introduced into CAT- and RUNX3- expressing Hep3B. (A) Cell lysates were collected 48 h after transfection. Immunoblot analyses were performed using antibodies against RUNX3, TWIST1, E-cadherin, N-cadherin, and vimentin. Immunoblotting for α-actin levels was used to verify equal loading of cellular proteins.

Representative blots of more than 3 independent experiments are shown. (B) Cell migration activities were measured as described in the Material and Methods (mock, white bars; RUNX3, black bars). Results are normalized to data for GFP (control) transfected CAT-expressing Hep3B cells. Data represent the mean ± SE of more than 3 independent experiments, each performed in triplicate. n.s., $P > 0.05$; **, $P < 0.01$ (versus data for mock-transfected cells); Student's *t* test.

Fig. 5. Effect of JAG1 stimulation on epithelial-mesenchymal transition (EMT) markers. CMV-driven eukaryotic expression constructs for green fluorescent protein (GFP; control) and TWIST1 were transfected into CAT- and/or RUNX3- expressing Hep3B. Cell lysates were collected 48 h after transfection. Immunoblot analyses were performed using antibodies against RUNX3, E-cadherin, N-cadherin, and vimentin. Immunoblotting for α-actin levels was used to verify equal loading of cellular proteins. Representative blots of more than 3 independent experiments are shown.

Fig. 6. Correlations between RUNX3 expression and epithelial-mesenchymal transition (EMT) markers in human HCC

(A) The images show the immunohistochemical staining of E-cadherin (a, protein score of 0; b, protein score of 3) and N-cadherin (c, protein score of 0; d, protein score of 3). Bar = 100 μm.

(B,C) RUNX3, E-cadherin, N-cadherin, and TWIST1 protein expression were assessed by immunohistochemical analysis in human HCC tissues and corresponding tumor-free

sections. Plots of the E-cadherin (B) and N-cadherin (C) expression score are shown compared with the RUNX3 expression score. (D) Correlations between RUNX3 expression and EMT markers were analyzed using publicly available microarray data sets (www.oncomine.org). RUNX3, E-cadherin, N-cadherin, vimentin, and JAG1 expression are plotted. The data are shown as arbitrary expression values. A 95% tolerance ellipse for each pair of variables was calculated and plotted.

Supplemental Fig. 1. Morphological study of RUNX3-expressing hepatocellular carcinoma (HCC) cell lines. Eukaryotic expression constructs for CAT (mock) and RUNX3 were introduced into Huh7 and SK-Hep1 cell lines. After a 24-h incubation, micrographs were taken by phase-contrast microscopy. The micrographs are representative fields from 3 independent experiments. Bar = 100 μm.

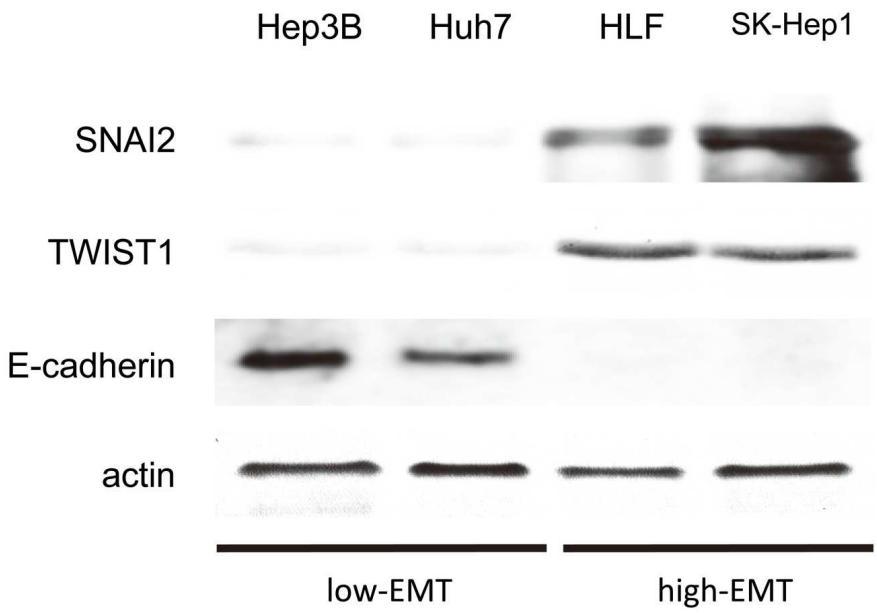

Fig. 1. Expression of epithelial-mesenchymal transition (EMT) inducers in hepatocellular carcinoma (HCC) cell lines. Immunoblot analyses were performed using antibodies against SNAI2, TWIST1, and E-cadherin. Immunoblotting for α-actin levels was used to verify equal loading of cellular proteins. HCC cell lines were divided into 2 groups according to EMT-inducer SNAI2 and TWIST1expression. Representative blots of more than 3 independent experiments are shown.
125x98mm (300 x 300 DPI)

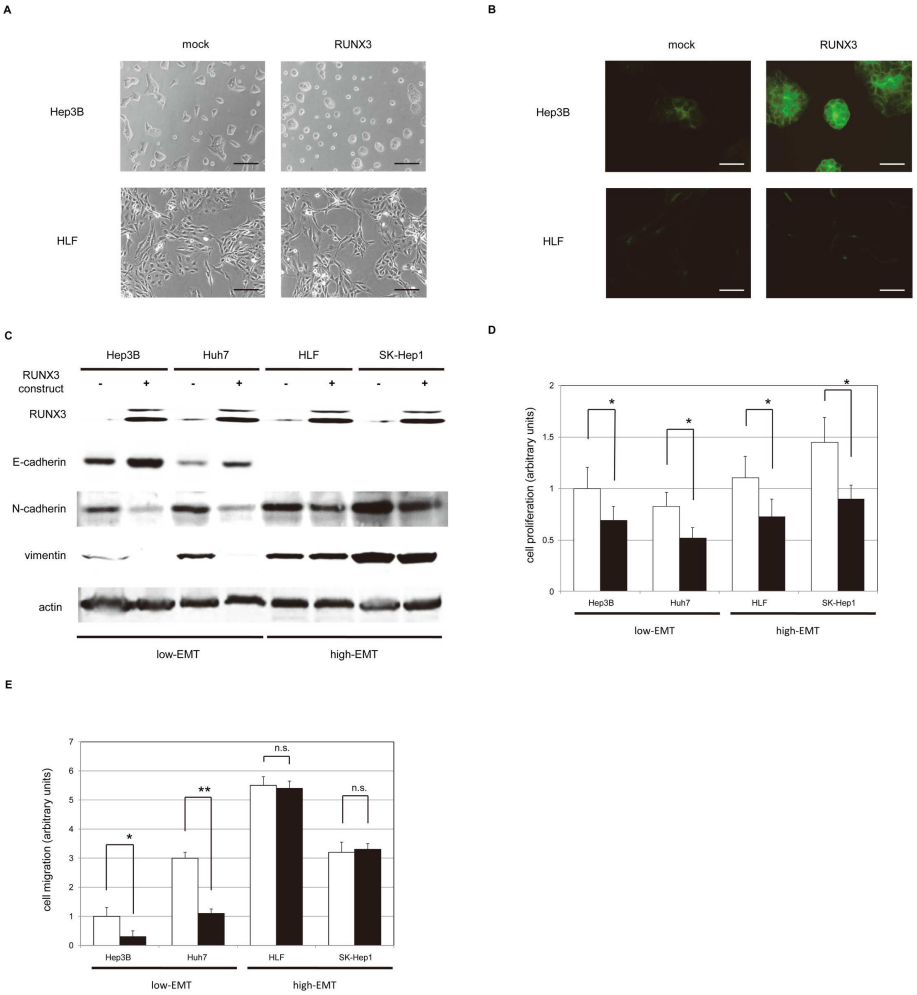

Fig. 2. Ectopic RUNX3 protein expression in hepatocellular carcinoma (HCC) cell lines. Eukaryotic expression constructs for CAT (mock) and RUNX3 were introduced into Hep3B, Huh7, HLF, and SK-Hep1 cell lines. After a 24-h quiescence, cells were used for the experiments in the presence of 10% FBS. (A) Micrographs were taken by phase-contrast microscopy. The micrographs are representative of 3 independent experiments. Bar = 100 μm. (B) Immunocytochemical analysis was performed using antibody against E-cadherin. The micrographs are representative of 3 independent experiments. Bar = 40 μm. (C) Immunoblot analyses were performed using antibodies against RUNX3, E-cadherin, N-cadherin, and vimentin. Immunoblotting for α-actin levels was used to verify equal loading of cellular proteins. Representative blots of more than 3 independent studies are shown. (D) Cell proliferation activity was measured by MTT assay (mock, white bars; RUNX3, black bars). (E) Cell migration activity was measured as described in the Material and Methods (mock, white bars; RUNX3, black bars). (D, E) All results were normalized to cell proliferation and migration activity for CAT-expressing Hep3B cells. Data represent the mean ± SE of more than 3 independent experiments, each performed in triplicate. n.s., $P > 0.05$; *, $P < 0.05$; **, $P < 0.01$ (versus data for mock-transfected Hep3B); Student's t test.
204x206mm (300 x 300 DPI)

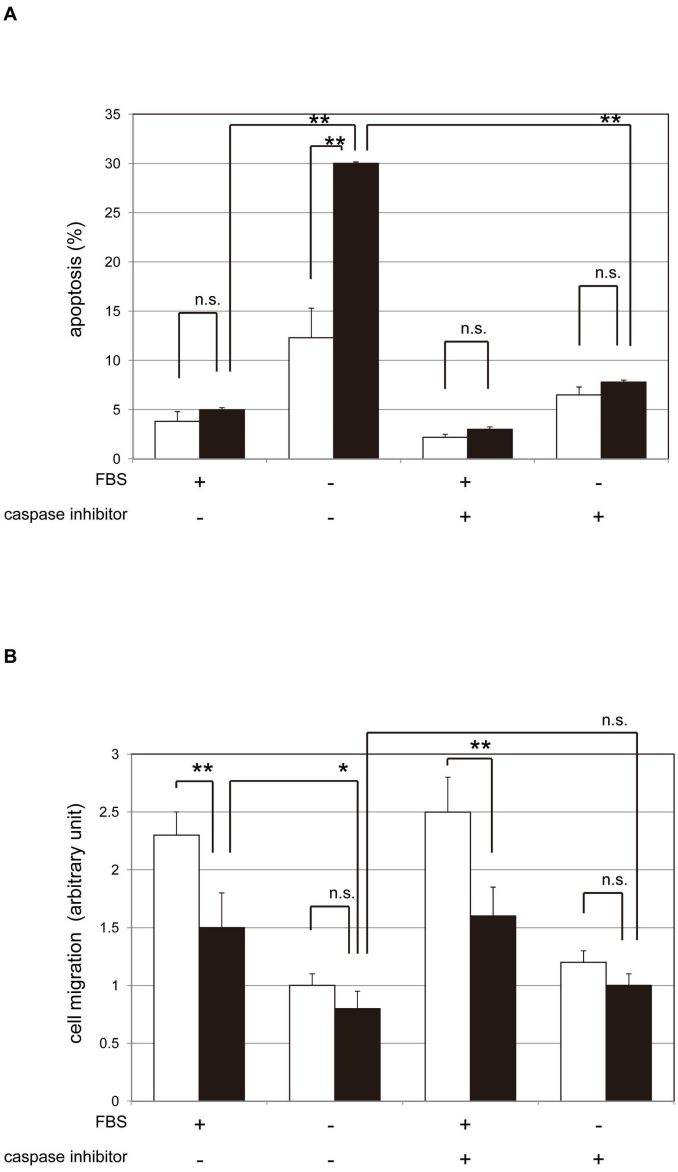

Fig. 3. Effect of an apoptosis inhibitor. Hep3B cells were cultured on glass chamber slides and quiesced, then treated with or without caspase inhibitor IV (100 μM) and 10% fetal bovine serum. (A) Apoptosis was quantified using the DAPI apoptosis detection assay (mock, white bars; RUNX3, black bars). Results are expressed as percent apoptotic cells. Data represent the mean ± SE of more than 3 independent experiments, each performed in triplicate. n.s., $P > 0.05$; **, $P < 0.01$ (versus data for mock-transfected cells); Student's t test. (B) Cell migration activities were measured as described in the Material and Methods (mock, white bars; RUNX3, black bars). All results are normalized to data for untreated control cells. Data represent the mean ± SE of more than 3 independent experiments, each performed in triplicate. n.s., $P > 0.05$; *, $P < 0.05$; **, $P < 0.01$ (versus data for mock-transfected cells); Student's t test.
178x278mm (300 x 300 DPI)

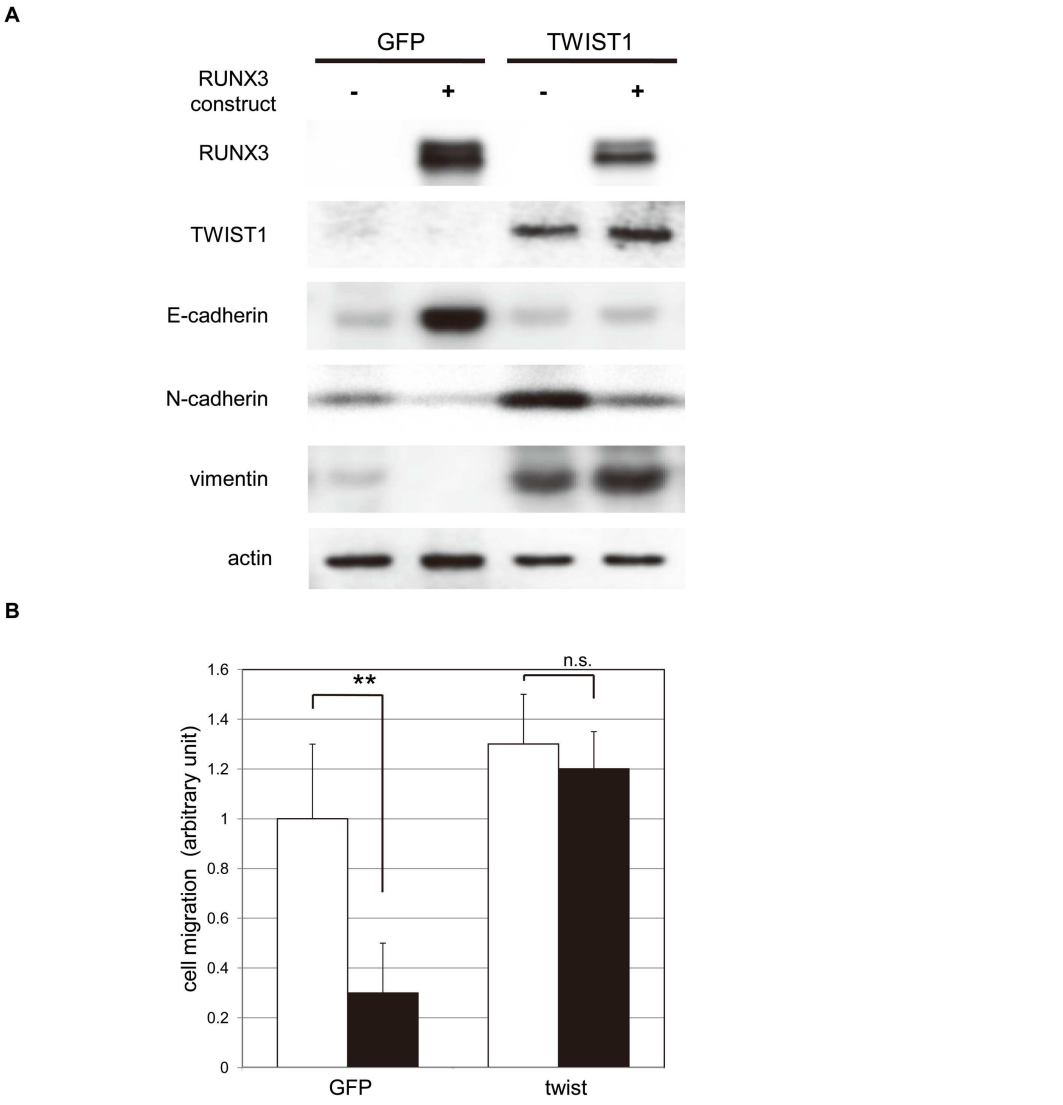

Fig. 4. Effect of TWIST1 expression on epithelial-mesenchymal transition (EMT) markers. CMV-driven eukaryotic expression constructs for green fluorescent protein (GFP; control) and TWIST1 were introduced into CAT- and RUNX3- expressing Hep3B. (A) Cell lysates were collected 48 h after transfection. Immunoblot analyses were performed using antibodies against RUNX3, TWIST1, E-cadherin, N-cadherin, and vimentin. Immunoblotting for α-actin levels was used to verify equal loading of cellular proteins. Representative blots of more than 3 independent experiments are shown. (B) Cell migration activities were measured as described in the Material and Methods (mock, white bars; RUNX3, black bars). Results are normalized to data for GFP (control) transfected CAT-expressing Hep3B cells. Data represent the mean ± SE of more than 3 independent experiments, each performed in triplicate. n.s., $P > 0.05$; **, $P < 0.01$ (versus data for mock-transfected cells); Student's t test.
223x247mm (300 x 300 DPI)

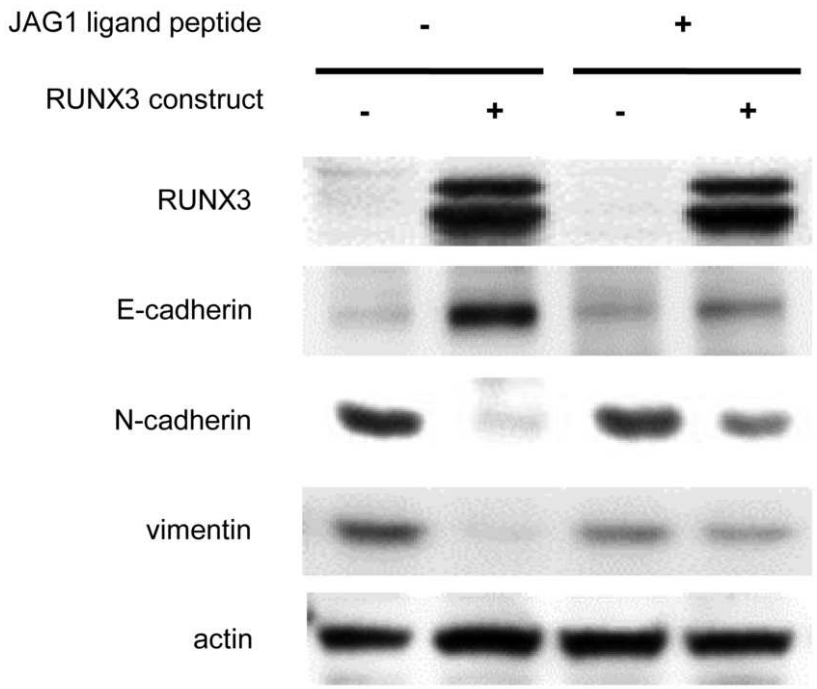

Fig. 5. Effect of JAG1 stimulation on epithelial-mesenchymal transition (EMT) markers. CMV-driven eukaryotic expression constructs for green fluorescent protein (GFP; control) and TWIST1 were transfected into CAT- and/or RUNX3- expressing Hep3B. Cell lysates were collected 48 h after transfection. Immunoblot analyses were performed using antibodies against RUNX3, E-cadherin, N-cadherin, and vimentin. Immunoblotting for α-actin levels was used to verify equal loading of cellular proteins. Representative blots of more than 3 independent experiments are shown.
87x76mm (300 x 300 DPI)

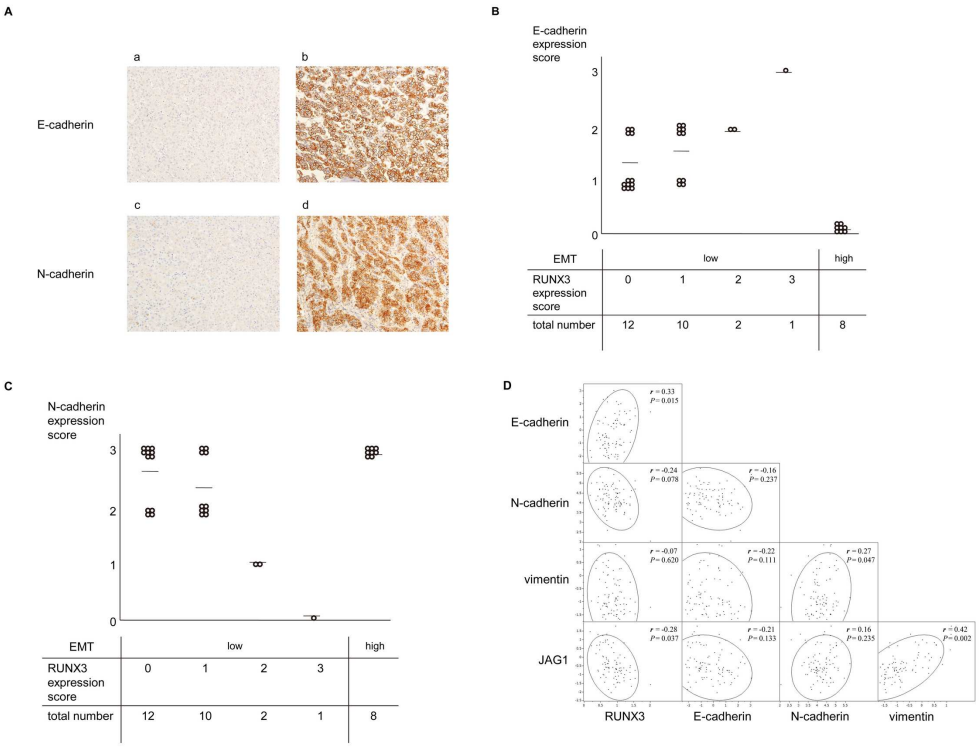

Fig. 6. Correlations between RUNX3 expression and epithelial-mesenchymal transition (EMT) markers in human HCC

(A) The images show the immunohistochemical staining of E-cadherin (a, protein score of 0; b, protein score of 3) and N-cadherin (c, protein score of 0; d, protein score of 3). Bar = 100 μm. (B,C) RUNX3, E-cadherin, N-cadherin, and TWIST1 protein expression were assessed by immunohistochemical analysis in human HCC tissues and corresponding tumor-free sections. Plots of the E-cadherin (B) and N-cadherin (C) expression score are shown compared with the RUNX3 expression score. (D) Correlations between RUNX3 expression and EMT markers were analyzed using publicly available microarray data sets (www.oncomine.org). RUNX3, E-cadherin, N-cadherin, vimentin, and JAG1 expression are plotted. The data are shown as arbitrary expression values. A 95% tolerance ellipse for each pair of variables was calculated and plotted.

194x148mm (300 x 300 DPI)

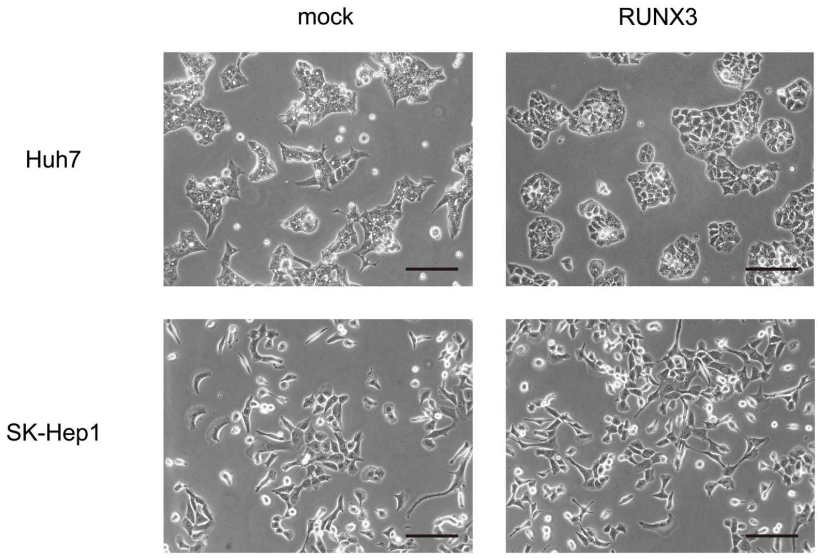

Supplemental Figure 1

Supplemental Fig. 1. Morphological study of RUNX3-expressing hepatocellular carcinoma (HCC) cell lines. Eukaryotic expression constructs for CAT (mock) and RUNX3 were introduced into Huh7 and SK-Hep1 cell lines. After a 24-h incubation, micrographs were taken by phase-contrast microscopy. The micrographs are representative fields from 3 independent experiments. Bar = 100 μm.
163x112mm (300 x 300 DPI)

Supplemental Table 1 TWIST1 and RUNX3 expression levels and clinicopathological features.

EMT (TWIST1)			Low		High
RUNX3 expression score	0	1	2	3	
Number	12	10	2	1	8
pTNM stage					
Stage I	2	1	0	0	2
Stage II	1	6	1	0	4
Stage IIIA	9	3	1	1	2
Stage IIIB	0	0	0	0	0
Stage IV	0	0	0	0	0
Distant metastasis					
M0	12	10	2	1	8
M1	0	0	0	0	0
Portal vein invasion					
Absent	8	9	2	1	5
Present	4	1	0	0	3